

## Article

# Development of Chitosan-Based Films Incorporated with Chestnut Flower Essential Oil That Possess Good Anti-Ultraviolet Radiation and Antibacterial Effects for Banana Storage

Yanfei Liu <sup>1,2,3</sup>, Jingyuan Zhang <sup>1,2,3</sup>, Fei Peng <sup>1,2,3</sup>, Kui Niu <sup>1,2,3</sup>, Wenlong Hou <sup>1,2,3</sup>, Bin Du <sup>1,2,3,\*</sup>   
and Yuedong Yang <sup>1,2,3,\*</sup>

<sup>1</sup> Hebei Key Laboratory of Natural Products Activity Components and Function, Hebei Normal University of Science and Technology, Qinhuangdao 066004, China; hbkslyf@163.com (Y.L.); zjy320323@163.com (J.Z.); flyer5212528@163.com (F.P.); niukui007@163.com (K.N.); wenlonghou@126.com (W.H.)

<sup>2</sup> Hebei Collaborative Innovation Center of Chestnut Industry, Hebei Normal University of Science and Technology, Qinhuangdao 066004, China

<sup>3</sup> Ministry of Education Engineering Research Center of Chestnut Industry Technology, Hebei Normal University of Science and Technology, Qinhuangdao 066004, China

\* Correspondence: bindufood@aliyun.com (B.D.); kycyyd@126.com (Y.Y.)

**Abstract:** New and valuable packaging materials, with high biocompatibility and biodegradability, have garnered attention in recent years. The aim of this study was to investigate the physicochemical characterization and biological activities of chitosan (CH)-based composite films with the incorporation of chestnut flower essential oil (CFEO). The composite films were prepared by the casting method and characterized in terms of structural, morphological, and mechanical properties via FT-IR, XRD, UV, SEM, AFM, and TGA. Antibacterial properties were investigated using *Staphylococcus aureus*, *Escherichia coli*, and *Calleotrichum musae*. Antioxidant capabilities were measured by DPPH assay. The results proved the significantly increased water vapor permeability (WVP), heat resistance, and antibacterial and antioxidant capabilities of CH-CFEO films. The incorporation of CH and CFEO enhanced UV blocking, which made the film shield almost all UV light. Films with a tensile strength of  $6.37 \pm 0.41$  MPa and an elongation at break of  $22.57 \pm 0.35\%$  were obtained with  $6 \text{ mg mL}^{-1}$  of CFEO. Subsequently, banana preservation experiments also confirmed that the composite films could effectively extend shelf life through reducing weight loss. These desirable performances enable our newly developed composite films to be a remarkable packaging material to become alternatives to traditional petroleum-based food-packaging materials and solve the fresh fruit preservation dilemma.

**Keywords:** chestnut flower essential oil; composite film; chitosan; antibacterial activity; fruit-packaging applications



**Citation:** Liu, Y.; Zhang, J.; Peng, F.; Niu, K.; Hou, W.; Du, B.; Yang, Y. Development of Chitosan-Based Films Incorporated with Chestnut Flower Essential Oil That Possess Good Anti-Ultraviolet Radiation and Antibacterial Effects for Banana Storage. *Coatings* **2024**, *14*, 548. <https://doi.org/10.3390/coatings14050548>

Academic Editors: Domingo Martínez-Romero, Huertas María Díaz-Mula and Juan Miguel Valverde

Received: 20 March 2024

Revised: 22 April 2024

Accepted: 24 April 2024

Published: 27 April 2024



**Copyright:** © 2024 by the authors. Licensee MDPI, Basel, Switzerland. This article is an open access article distributed under the terms and conditions of the Creative Commons Attribution (CC BY) license (<https://creativecommons.org/licenses/by/4.0/>).

## 1. Introduction

With the remarkable demand for fruits and vegetables, antibacterial packaging has been produced to control or inhibit microbial growth and retain food quality and safety. Food packaging is an integral part of the food production process, and food is packaged to protect it from microbial attack, mechanical damage, chemical deterioration, ultraviolet radiation, etc. Most food packaging is currently made from petroleum-based synthetic plastics, which can have a negative impact on the environment, causing soil and water contamination and harming aquatic organisms [1]. As a result, some researchers have focused their attention on other areas, such as biopolymers, which are gradually becoming an alternative to synthetic plastics due to a number of advantages, such as biodegradability, biocompatibility, environmental friendliness, and non-toxicity [2,3]. However, they also have some drawbacks, such as poor mechanical, thermal, barrier, and film-forming

properties. These disadvantages of biopolymers can be improved by structural modification, blending of two or more biopolymers. Existing oil-based packaging materials cause serious environmental problems owing to their non-degradable properties, which will finally threaten the health of people [4]. In particular, the application of natural essential oils (EOs) as antimicrobial agents promisingly delays the growth of pathogenic microbes. Emerging studies have increased due to the potential of some active packaging to suppress food spoilage and extend shelf life, especially active packaging containing natural polymers with potent antioxidant and antibacterial properties [5,6]. Composite films can be fabricated from natural polymers, such as chitosan, cellulose derivatives, collagen, elastin, and starch, and used as packaging materials to extend shelf life and product safety [7]. Chitosan (CH) is a naturally abundant cationic polymer used for antibacterial packaging to meet the growing needs of safe and biodegradable packaging [8,9]. Therefore, edible chitosan coatings and films incorporated with EOs have expanded the general applications of antimicrobial packaging in fruits and vegetables [10].

Chitosan is a linear cationic polysaccharide consisting of d-glucosamine and n-acetyl-d-glucosamine monomer-linked  $\beta$ -(1 $\rightarrow$ 4), which is chemically composed of cellulose-based biopolymers derived by deacetylating chitin [11]. CH is a natural biomaterial widely used in agriculture, food packaging, biomedical engineering, and other fields because of its non-toxicity, degradability, wide availability, reproducibility, good biocompatibility, broad-spectrum antibacterial capacity, and excellent film-forming ability [12–15]. Although CH has great potential as an antibacterial packaging material [16], it still has disadvantages as a film and coating, such as insufficient UV blocking and poor antioxidant and antimicrobial properties. And alone, it has little effect on common strains of microorganisms that cause spoilage [8]. To overcome these shortcomings, some researchers have combined chitosan films with natural compounds (e.g., plant EOs, organic acids, or fruit extracts) for the fabrication of antimicrobial, biodegradable packaging in combination with film [17–20]. Furthermore, UV exposure accelerates the aging and degradation of these films and thus significantly reduces their lifetime [21]. Therefore, natural UV-resistant additives, such as EOs, for effective UV protection are urgently needed.

The components in EOs are mainly secondary metabolites, which are volatile aromatic products extracted from plant species [22]. Currently, some studies have demonstrated that EOs have biological activities, such as antibacterial [23,24], antifungal [25,26], and antiparasitic [27] activities. Consequently, various researchers have incorporated EOs into chitosan films to enhance the mechanical and biological properties of the chitosan films. Shahbazi et al. reported that the addition of EOs to chitosan films has a possible antibacterial effect against both Gram-positive and Gram-negative bacteria [28]. Wang et al. demonstrated that the synergistic effect of chitosan and cinnamon oil increases antibacterial activity against *Escherichia coli*, *Staphylococcus aureus*, *Aspergillus oryzae*, and *Penicillium yangdii* and that the addition of 0.4% cinnamon EOs enhances the antibacterial performance of chitosan films against a variety of bacteria [29,30]. However, there are few reports on the combination of chestnut flower essential oil (CFEO) with chitosan to prepare composite films. Chestnut flowers are the male inflorescences of chestnut trees, which are long in shape. Chestnut trees are monoecious, and the number of male flowers during flowering is large, far exceeding the pollination needs of female flowers, so a large number of chestnut male flowers cannot be used effectively. It is generally believed that chestnut flowers contain not only amino acids, proteins, reducing sugars, crude fiber, and other nutrients but also flavonoids, volatile oils, and other bioactive substances [31].

Banana is an important and popular fruit due to its good flavor and high nutritional value. However, it is susceptible to physiological aging and anthracnose infections during storage processes [32,33]. It is highly urgent to explore a simple and effective strategy to increase the shelf life of time-sensitive bananas, which are susceptible to spoilage over time.

Herein, in this study, a chitosan–chestnut flower extract composite membrane was prepared by using chitosan as the matrix and chestnut flower essential oil as the material. The films were characterized by FITR, XRD, UV, TGA, and SEM, and their mechanical proper-

ties, antioxidant and antibacterial activities, and banana preservation applications were also investigated. This research will underpin our understanding of the development of novel composite films, providing valuable information for fruit shelf life practical applications.

## 2. Materials and Methods

### 2.1. Materials

Fresh bananas were purchased from a local supermarket in Qinhuangdao (these bananas were from one batch and had same freshness). Chitosan (CH; degree of deacetylation 80%–90%,  $M_W = 50,000$  Da) was purchased from Shanghai Eon Chemical Technology Co; glycerol and DMSO were supplied by Tianjin Oubokai Company; 2,2-diphenyl-1-picrylhydrazyl (DPPH) was supplied by Shanghai Yuanye Biotechnology Co; acetic acid was purchased from Tianjin Guangfu Technology Development Company; *Escherichia coli* (ATCC 25922), *Staphylococcus aureus* (ATCC 23656), and *Calletotrichum musae* (ATCC 31244) were bought from Shanghai Yixin Biotechnology Company (Shanghai, China); and *Castanea mollissima* Blume flower was obtained from Qinglong County, Qinhuangdao City. The chemicals used throughout the experiment were of analytical grade, and the water used for the experiment was deionized water.

### 2.2. Preparation of the CH-CFEO Composite Film

First, CFEO was extracted from the target using a plant essential oil extraction device (Shunfu Technology Co., Ltd., Beijing, China), with n-butane as the solvent. Geraniol and menthol are the main components in CFEO and account for its antibacterial activity, as shown in our previously published work [31]. Next, 1.2 g of chitosan was mixed with 1% (v/v) glacial acetic acid, and the temperature of the thermostat stirrer was set to 55 °C. After the mixed solution was stirred in the thermostat stirrer for 1 h, 1 mL of glycerol was added to it and continuously stirred for 30 min, and the mixed solution was left to stand overnight. CFEO of different concentrations (6, 8, 10, 20, 40 mg/mL) was dissolved in 1 mL of DMSO, and the film-forming solution was mixed well with the dissolved CFEO (fixed to 10 mL), poured into a mill, and dried in an oven at 50 °C to obtain a composite film.

### 2.3. Characterization of Composite Films

#### 2.3.1. Thickness and Mechanical Properties

The thickness of the prepared films was measured using a vernier caliper (Suzhou Guoliang Co., Suzhou, China). The measured values at 5 random locations were recorded, and the average value was taken as the final result.

According to the ISO 527-2012 standard method with appropriate modifications [34], tensile strength (TS) and elongation at break (EB) were tested using a universal material-testing machine (INSPEK TABLE100, Ismaning, Germany). Thin film sample strips (50 mm × 20 mm) were stored at a room temperature of 23 °C, a humidity of 50% adjusted for 4 days, test type 2, a gauge distance of 50 mm, and a speed of 5 mm/min. TS was calculated by dividing the maximum force with the initial cross-sectional area of the film; EB (%) was calculated by dividing the film elongation at break with the initial gauge length of the specimen. Each sample was tested at least 3 times in parallel (1).

$$EB = \frac{L_1 - L_0}{L_1} \times 100\% \quad (1)$$

The initial and final lengths of the film were denoted as  $L_0$  and  $L_1$ , respectively.

#### 2.3.2. Fourier Transform Infrared Spectroscopy (FT-IR)

The FT-IR spectra of the film samples were obtained using a spectrometer (Tensor27, Bruker Corporation, Karlsruhe, Germany). A total of 32 scans were carried out at a spectrum wavenumber range of 400–4000  $\text{cm}^{-1}$ .

### 2.3.3. Transmittance of the Composite Films

The optical transmittance of the composite films was measured from 200 to 800 nm by a UV-Vis spectrophotometer (U-4100, Hitachi Limited, Tokyo, Japan) [35].

### 2.3.4. Atomic Force Microscopy (AFM)

Atomic force microscopy (AFM) images were obtained with a Dimension Icon XR atomic force microscope (Bruker, Santa Barbara, CA, USA) working in the air in peak force tapping (PFT) mode using standard silicon cantilevers (Bruker) with a tip radius below 10 nm. Before measurements, each sample was cut into small pieces and glued to a smooth silicon wafer.

### 2.3.5. Appearance and Microstructure of Films

The appearance of CH-CFEO composite films was captured by a high-resolution camera. The microstructure of the films was investigated by scanning electron microscopy (SEM) (SU 8010, Hitachi Limited, Tokyo, Japan). Moisture was removed from the films and they were sputter-coated with gold to enhance conductivity. Subsequently, the microstructure of the films was observed at a magnification of 200× and 500×.

### 2.3.6. X-ray Diffraction (XRD) Analysis

The XRD patterns of the film samples were recorded on a wide-angle X-ray diffractometer (D/max-2500 vk/pc; Rigaku Corporation, Tokyo, Japan) under an area detector operating at a voltage of 40 kV and a current of 200 mA using Cu/K $\alpha$  radiation. The scanning speed was 8° min<sup>-1</sup> in a 2 $\theta$  range from 10 to 80°.

### 2.3.7. Water Vapor Permeability (WVP)

To evaluate the WVP of the formulated films, we applied the methods of Zhang et al. [36] and Liu et al. [37] with some modifications. Film samples were first sealed onto 15 mL centrifuge tubes that contained calcium chloride and then were stored at 20 °C in a desiccator, together with a beaker filled with distilled water. The film-sealed centrifuge tubes were weighed after 24 h, and the WVP was calculated as follows (2):

$$WVP(\text{gm}^{-1}\text{h}^{-1}\text{Pa}^{-1}) = \frac{w \times d}{t \times A \times \Delta P} \quad (2)$$

where  $W$  (g) is the bottle weight difference,  $t$  (h) is the permeation time,  $d$  is the average thickness of the film (mm),  $A$  (m<sup>2</sup>) is the exposed film area, and  $\Delta P$  (Pa) is the vapor pressure difference.

### 2.3.8. Moisture Content and Water Solubility

Film samples (4 × 4 cm<sup>2</sup>) were prepared and weighed ( $W_s$ ) and then dried in an oven at 105 °C until a constant weight was reached ( $W_i$ ) [38]. The film solubility (MS %) was calculated by using Equation (3):

$$MS = \frac{W_s - W_i}{W_s} \times 100\% \quad (3)$$

where  $W_i$  is the weight of the sample after the drying process (g) and  $W_s$  is the initial dry weight of the sample (g).

The WS of the films was measured by the method in a previously published work [39]. First, the initial weight of each film was defined as  $W_1$ . The film was then immersed in 50 mL of distilled water for 1 h at 30 °C. The undissolved film was dried at 105 °C for 24 h and then weighed to obtain the dry weight ( $W_2$ ). The WS of the prepared films was calculated from Equation (4).

$$W_S = \frac{W_1 - W_2}{W_1} \times 100\% \quad (4)$$

### 2.3.9. Thermogravimetric Analysis (TGA)

TGA of the samples was performed by a thermogravimetric analyzer (STA409PC, PYRIS 1; NETZSCH Gertebau GmbH, Selb, Germany) [40]. Each film sample (3–5 mg) was sealed in an aluminum plate and heated from 10 °C to 800 °C at a heating rate of 10 °C/min in a nitrogen atmosphere (20 mL/min).

### 2.3.10. Antioxidant Activity of Composite Films

The antioxidant activity of the films was assessed using a 2,2-biphenyl-1-picrylglycyl (DPPH) radical scavenging method [41,42]. The films were cut into 3 cm × 3 cm squares and then placed in a fatty food simulator system (95% alcohol system). Next, 3 mL of the simulated solution containing the active substance was mixed with 1 mL of DPPH ethanol solvent and reacted in the dark for 30 min. The absorbance of the solution was measured by a microplate reader (SpectraMax 190; Molecular Devices, Shanghai, China) at 517 nm, and the measurements were repeated three times. The scavenging rate of free radicals was determined using Equation (5).

$$DPPH(\%) = \frac{A_0 - A_s}{A_0} \times 100\% \quad (5)$$

where  $A_0$  is the absorbance of the control and  $A_s$  is the absorbance of the film sample.

## 2.4. Antibacterial and Antifungal Activities

### 2.4.1. Antibacterial Activities

The antibacterial activity of the films against *Staphylococcus aureus* and *Escherichia coli* was determined using the paper diffusion method reported by Lei et al. with appropriate modifications [43]. First, 11.75 g of nutrient broth was dissolved in 500 mL of distilled water, simmered with thorough stirring, and then sterilized in an autoclave at 121 °C, after which the medium was poured in Petri dishes and cooled. Next, *Staphylococcus aureus* and *Escherichia coli* diluted to a certain concentration ( $10^5$  CFU/mL) were spread onto the medium. A CH blank film with different concentrations of CFEO (6, 8, 10, 20, 40 mg/mL) was spread 7 mm onto the planted medium, and 10% DMSO and 1 µg/mL of levofloxacin were used as negative and positive controls, respectively. The medium was incubated at 37 °C for 24 h, and the inhibition circle of different concentrations of the composite film was measured at the end of the experiment, and the test was measured three times in parallel.

### 2.4.2. Evaluation of the Effects of CH-CFEO on *Calleotrichum musae* Mycelial Growth

The antifungal activity of the films was determined according to the method published by Yang et al. [33]. The paper disk diffusion method was used in this study. The effects of CH-CFEO on the radial mycelial growth of *C. musae* isolates were assessed with a solid media dilution procedure [41]. *C. musae* isolates were grown on PDA for 5 days ( $25 \pm 0.5$  °C), and mycelial agar plugs (5 mm diameter) were taken from the margin of the cultures, transferred to the center of a Petri dish with PDA + CH (50 µg/mL, 100 µg/mL) or CFEO (0.03% w/v, 0.06% w/v), and incubated at  $25 \pm 0.5$  °C. PDA without CH or CFEO was tested as a negative control. Measurements of the orthogonal diameters of fungal colonies were taken after 5 days or until the negative control Petri dishes were fully covered with fungal mycelia.

The percentage of mycelial growth inhibition (MGI%) was calculated with Equation (6):

$$MGI(\%) = \frac{C - T}{C} \times 100\% \quad (6)$$

where C is the colony diameter in the control assay and T is the colony diameter in PDA with CH-CFEO at the examined concentration.

## 2.5. Effect of Developed Films on Banana Quality

### 2.5.1. Sample Preparation

Bananas with the same freshness were placed in sterilized polypropylene boxes, covered with a laminated film, and sealed with petroleum jelly. Each group of fruits was weighed regularly and expressed in terms of weight reduction [42]. Bananas without a composite film were used as the control group.

### 2.5.2. Weight Loss

The specific means of the treatment of bananas during the experiment were as follows: First, the bananas bought were washed with water and then dried with paper. Next, the polyethylene box was sterilized with alcohol, the bananas were put into the box without a film as a blank control, and different concentrations of the essential oil of *Platanthera*—chitosan composite film were coated on the polyethylene box as an experimental group under the experimental conditions of a humidity of 100% and a temperature of 25 °C for the test. The weight loss and apparent morphology of the bananas were recorded on different days. To evaluate the moisture loss, the bananas were weighed before ( $W_0$ ) and after ( $W_1$ ) the test, and then, we applied the following Equation (7):

$$\text{Weight Loss(\%)} = \frac{W_0 - W_1}{W_0} \times 100\% \quad (7)$$

## 2.6. Statistical Analysis

All experiments were performed at least in triplicate and presented as means  $\pm$  standard deviations (SDs). SPSS 20.0 software (SPSS, Inc., Chicago, IL, USA) was used to perform one-way analysis of variance, and significant differences ( $p < 0.05$ ) among samples were analyzed using Duncan's multiple range tests.

## 3. Results

### 3.1. Thickness, Water Solubility, Water Content and WVP Rate of Composite Films

Table 1 summarizes the results of the physical and chemical properties of the film. Compared with the chitosan control film, the thickness of the CFEO composite film increased slightly with different concentrations. When the essential oil concentration reached 40 mg/mL, the thickness of the composite film was 0.12 mm, which may have combined with the alcohols in CFEO with CH, resulting in a tighter structure of the composite membrane [43], and because chitosan contains a large number of hydroxyl groups, this makes the distance between chitosan molecules narrower and the structure tighter, thus increasing the film thickness [44,45]. For the water solubility of the film, the chitosan control membrane had the largest water solubility, and with the increase in the CFEO concentration, the water solubility of the film gradually decreased, and the lowest value was 20.05%, which is about half of that of the chitosan control film. The reason for the lower water solubility may be the hydrophobic nature of CFEO, which interacts less with water molecules, resulting in reduced water solubility. As a result, when the CFEO concentration increased, the moisture content of the film underwent a similar change [46,47]. The moisture permeability of the prepared films was observed using the WVP experiment. The WVP is a parameter that reflects water vapor adsorption, sorption and diffusion and plays an important role in food packaging [48]. With the increase in the essential oil concentration, the water vapor transmittance of the composite membrane decreased gradually; especially, when the concentration of CFEO was 40 mg/mL, the water vapor transmittance of the composite membrane was  $8.13 \times 10^{-7}$  ( $\text{g m}^{-1}\text{h}^{-1}\text{Pa}^{-1}$ ). The low WVP of the food-packaging films prevented moisture transfer between the food and its surroundings. Also, the thickness of the film played a vital part in its waterproof performance. Thicker films had lower WVP values because it took longer for water molecules to penetrate the films [49].

**Table 1.** Thickness, water solubility, water content, and water vapor transmission rate of composite films.

Sample (mg/mL)	Thickness (mm)	Water Solubility (%)	Water Content (%)	WVP ( $\text{gm}^{-1}\text{h}^{-1}\text{Pa}^{-1}$ )	Dry Films
CH	$0.06 \pm 0.01^b$	$49.01 \pm 0.44^a$	$70.68 \pm 0.46^c$	$1.36 \times 10^{-6} \pm 0.08^b$	
CH-6	$0.07 \pm 0.01^b$	$36.25 \pm 0.45^b$	$76.83 \pm 0.34^a$	$1.13 \times 10^{-6} \pm 0.08^b$	
CH-8	$0.07 \pm 0.01^b$	$37.17 \pm 0.34^b$	$73.17 \pm 0.35^b$	$1.37 \times 10^{-6} \pm 0.07^b$	
CH-10	$0.08 \pm 0.01^b$	$25.22 \pm 0.50^c$	$72.63 \pm 0.50^b$	$1.24 \times 10^{-6} \pm 0.09^b$	
CH-20	$0.10 \pm 0.02^{ab}$	$22.25 \pm 0.76^d$	$72.10 \pm 0.51^b$	$7.76 \times 10^{-7} \pm 0.44^a$	
CH-40	$0.12 \pm 0.01^a$	$19.90 \pm 0.97^e$	$60.16 \pm 0.57^d$	$8.13 \times 10^{-7} \pm 0.24^a$	

Note: The same letters are not significantly different at  $p < 0.05$ .

### 3.2. FT-IR Analysis

The infrared spectra of the composite films are shown in Figure 1a. The infrared spectral peak of the chitosan standard sample presented a wide band with a width of  $3375 \text{ cm}^{-1}$ , which belongs to OH tensile vibration, overlapping the amino tensile band in the same region. Studies have found that chitosan molecules contain a large amount of free hydroxyl groups and hydrogen, which can easily form intramolecular and intermolecular hydrogen bonds, forming the overall structure of the film [50]. C-H absorption peaks were at  $2983 \text{ cm}^{-1}$ , and C-O, n-H flexural vibration, C-N tensile, and C-O-C band stretching peaks at  $1517$ ,  $1403$ ,  $1264$ , and  $800 \text{ cm}^{-1}$ , respectively [51]. CFEO appeared at  $2923 \text{ cm}^{-1}$  with a sharp peak, possibly a tensile vibration of C-H on methyl [52]. After adding CFEO, the adsorption peak of the composite membrane did not shift significantly, indicating that there was no chemical reaction between chitosan and CFEO. FT-IR analysis confirmed that hydrogen bonds may have been formed between CH and CFEO, which limited the number of free OH groups interacting with water, resulting in lower WVP values [49]. The main reason is that after adding CFEO, more hydrogen bonds are formed between chitosan and CFEO, and the intermolecular force is enhanced, so it is more difficult for water molecules to enter the composite film. These findings indicated a decrease in the moisture permeability and water vapor permeability.

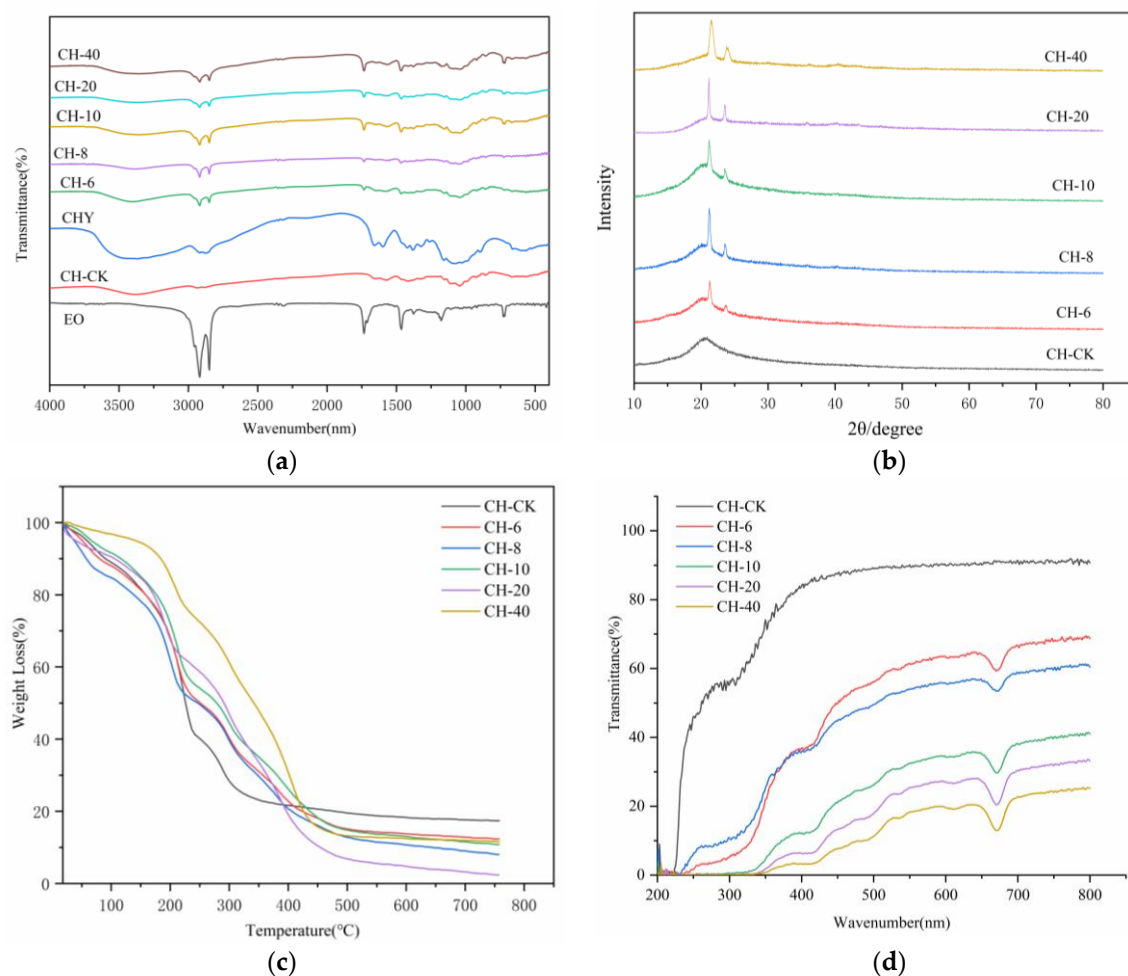


**Figure 1.** FT-IR (a), XRD (b), TGA (c), UV (d) results for composite films obtained with different concentrations of chestnut flower essential oil.

### 3.3. X-ray Diffraction (XRD)

The XRD patterns of the chitosan blank film and composite membranes with CFEO at different concentrations are shown in Figure 1b. The chitosan blank membrane presented a wide single peak at  $2\theta$  of about  $21^\circ$ , and its diffraction peak width and height were similar, which can be considered to be an amorphous structure [45,53]. When CFEO was added, independent and narrow spikes appeared on the XRD spectrum, and with the increase in the essential oil concentration, the height of the composite membrane spike increased, which indicated that the addition of CFEO would increase the crystallinity of the composite film. The composite film with CH-40 (mg/mL) had the highest crystallinity, which provided favorable evidence for the better mechanical properties and water resistance of the composite membrane. Usually, with an increase in crystallinity, the yield stress, strength, modulus, and hardness of the polymer increase, while the elongation at break and impact toughness reduce. This is because crystallinity increases after tightly ordered, low-porosity molecular chain arrangement, the intermolecular interaction force increases, and chain segment movement becomes difficult.

### 3.4. TGA

TGA curves presented in Figure 1c show the films' weight loss patterns upon heat treatment. The chitosan blank film had a large weight loss at about  $100\text{--}300^\circ\text{C}$ , indicating poor thermal stability, which is consistent with Zhang's research [54]. At a concentration of 6 mg/mL of CFEO, the first peak of the composite membrane appeared at  $90^\circ\text{C}$ , mainly due to the evaporation of water and volatile substances in the composite membrane. With

the increase in the chestnut flower essential oil concentration, the temperature of the first peak of the composite membrane was correspondingly transferred to a higher value; especially, when the essential oil concentration reached 40 mg/mL, its temperature reached 154 °C. The cause of these changes may be related to hydrophobic compounds in the film that hinder or delay the removal of water vapor and other volatiles [47], which is consistent with the results of the WS decline previously observed in these films. The second peak varied between 113 and 238 °C, which corresponds to the thermal decomposition of hydrogen bonds due to chemical adsorption, as well as the thermal decomposition of less volatile compounds, such as amino groups and glycerols of chitosan and organic acids. The third peak observed between 238 and 343 °C was primarily the chemical breakdown of the polymer. Overall, after the addition of CFEO, the thermal stability of the membrane improves, which helps the composite membrane to be used at higher temperatures.

### 3.5. UV

Ultraviolet (UV) radiation from the solar spectrum has a ubiquitous harmful impact on human health and other biological systems [55], and UV will induce the spoilage of food products. Developing UV-blocking packaging materials has been gradually gaining attention [56]. Figure 1d studies the UV and visible light blocking of thin films at 200–800 nm. It can be seen from the figure that the chitosan blank film had the highest transmittance and low UV-blocking performance. After adding essential oils, the transmittance was less than 20% in the wavelength range of 100–400 nm (ultraviolet region), indicating that they are highly UV-blocking materials. Similar findings have been reported in previous articles [57–59]. Especially, Ren et al. [60] prepared zein/chitosan/eugenol/curcumin active films with enhanced anti-UV ability. In the range of the visible light region, especially at 680 nm, the visible light transmittance of the control film was higher than that of the composite film, and when the concentration of CFEO increased sequentially, the transmittance of the composite film gradually decreased, and when the concentration of essential oil was 40 mg/mL, the transmittance was about 17%, which may be due to the opaque appearance of the composite film causing light scattering, hindering normal light transmission [61]. These results suggest that the film after the addition of chestnut flower essential oil can prevent the loss of nutrients and odor caused by direct exposure of certain foods to ultraviolet light. Moreover, there are some other reports presenting similar phenomena, in addition to this work. Roy and Rhim developed a bioactive binary composite film based on gelatin/chitosan incorporated with cinnamon EOs. The results showed that this film has good UV-blocking capacity [62].

### 3.6. The Mechanical Properties of Composite Films

The mechanical properties of packaging materials are important parameters for judging the quality of the packaging materials, mainly including tensile strength (TS) and elongation at break (EB) [62]. Tensile strength refers to the stress of the material to produce the maximum uniform plastic deformation, and elongation at break is an indicator of the toughness and elasticity of the material. From Figure 2, we can see that as the concentration of CFEO increased, the tensile strength of the film gradually decreased. The tensile strength of the chitosan blank film was 7.96 MPa, and when the essential oil concentration was 6 mg/mL (*w/v*), the tensile strength of the film was 6.66 Mpa, and the decrease was not obvious. With a further increase in the CFEO concentration, the tensile strength of the film decreased; especially, when the essential oil concentration was 40 mg/mL, the tensile strength of the film dropped to 0.84 MPa, which may be due to the cross-linking of some functional groups in chestnut flower essential oil with the functional groups in chitosan, weakening the interaction between the two molecules, resulting in a decrease in tensile strength. However, the reason may be that the size of CFEO affects the combination of the two, resulting in pores inside the film (which can be verified from the scanning electron microscopy cross section), so the tensile strength of the film decreases. For the elongation at break of the film, similar results to tensile strength appeared, but it is worth noting that

when the chestnut flower essential oil concentration was 8 mg/mL, the elongation at break of the film was 23.93%, which was slightly enhanced compared to that at the essential oil concentration of 6 mg/mL (22.82%).

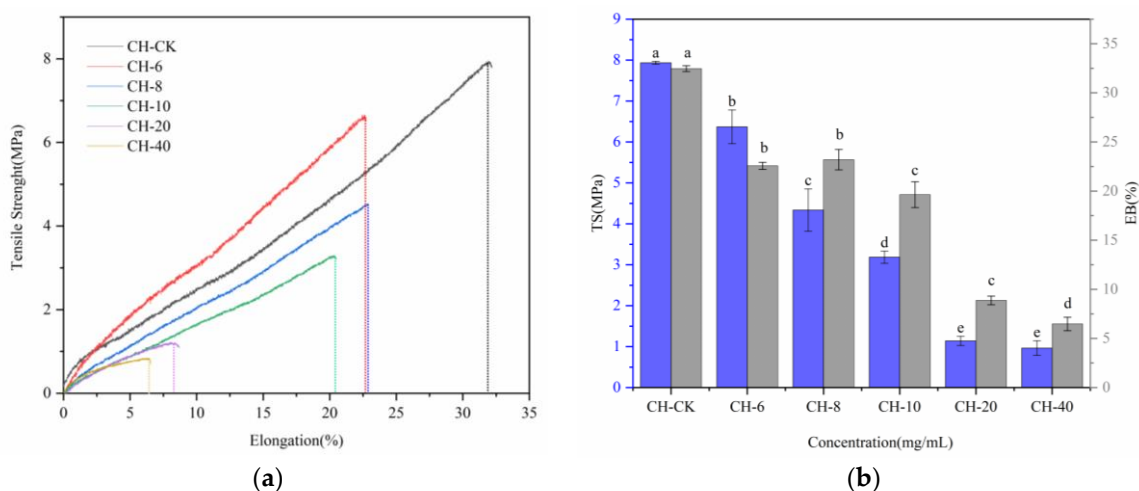


**Figure 2.** Stress–strain curve (a) and TS, EB (b) of composite films obtained with different concentrations of chestnut flower essential oil. The same letters are not significantly different at  $p < 0.05$ .

### 3.7. SEM and AFM of Prepared Films

The uniformity and network structure of the film-forming matrix were analyzed by SEM morphology (Figure 3). After adding different concentrations of chestnut flower essential oil, the surface and cross-sectional SEM micrographs of the film were obtained, as shown in the figure. From the scanning electron microscopy of the film, it can be seen that compared to the chitosan blank film, the surface and cross-sectional structure morphology of the film after adding chestnut flower essential oil had certain differences. The surface of the chitosan blank film was smooth and flat, and there were no holes, pores, and cracks on the cross section of the film. With the addition of chestnut flower essential oil, bulges appeared on the surface of the film, with small bulges formed one by one, probably due to the high hydrophobicity of chestnut flower essential oil. When the concentration of chestnut flower essential oil was 6 mg/mL, there were no obvious holes and cracks in the cross section of the film, indicating that the low concentration of chestnut flower essential oil could be evenly distributed in the membrane matrix, with strong interaction and good compatibility of each film-forming matrix. In addition, the cross-sectional structure morphology of the higher-concentration chitosan–chestnut flower essential oil film did not show more pores or cavities, but only folds appeared, indicating that the film-forming solution had good compatibility with chestnut flower essential oil, resulting in its structure becoming denser, which can also be used to explain the gradual decrease in the water vapor transmittance of the film with the increase in the essential oil concentration. However, the inclusion of CFEO resulted in greater roughness, as well as the formation of aggregates (Figure 3I–VI). The reason for such behavior can be seen in the high hydrophobicity of CFEO, which when introduced into a polymer solution tends to agglomerate, which results in visible cracks on the surface and cross-section images [63]. However, the differences between samples, which are shown in Figure 3IV–VI, may result from the differences in the water content of the CH-CFEO complexes, based on the water content (WC) results (Table 1). Moreover, the differences between samples in Figure 3II,III may result from uneven drying of the film.

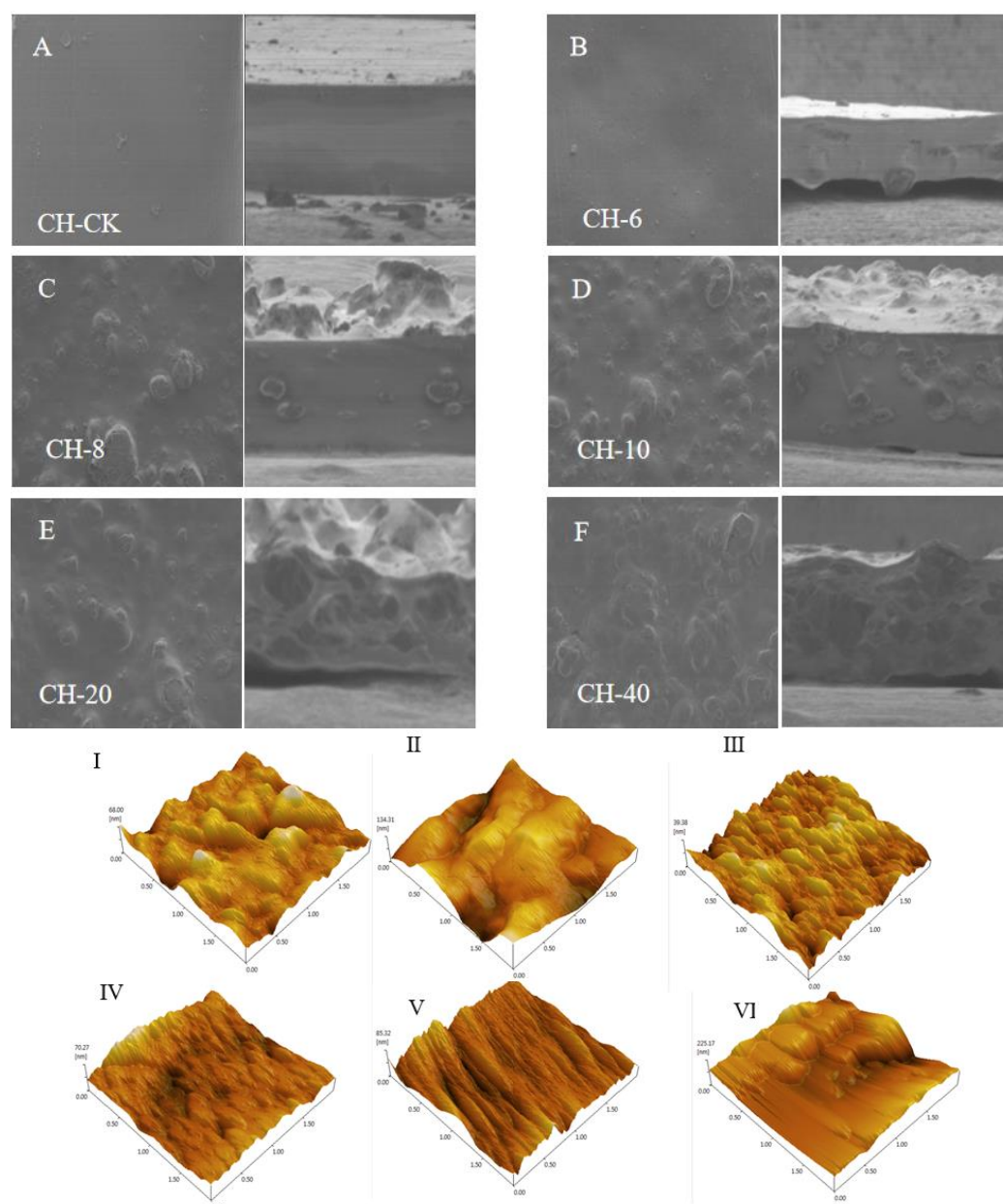


**Figure 3.** Scanning electron microscopy (SEM) images ( $\times 200$ ) and atomic force microscopy (AFM) images of composite films obtained with different concentrations of chestnut flower essential oil ((A–F) surface appearance: (A–F) cross-section appearance. AFM photos of (I) CH-CK, (II) CH-CFEO (6 mg/mL), (III) CH-CFEO (8 mg/mL), (IV) CH-CFEO (10 mg/mL), (V) CH-CFEO (20 mg/mL), and (VI) CH-CFEO (40 mg/mL)).

### 3.8. DPPH Assay for Free-Radical Scavenging

The DPPH free radical-scavenging percentage was used to determine the antioxidant activity of the films. The quenching and decolorization of DPPH free radicals result in their reduction to yellow diphenylpicryl hydrazine, with a corresponding reduction in the absorbance value [63]. The DPPH radical-scavenging capacity of the active composite films was determined (Figure 4). It was found that the scavenging capacity of the composite membrane increased as the CFEO content increased. The test results showed that with the increase in the CFEO concentration, the antioxidant capacity of the composite membrane gradually increased; especially, when the concentration of essential oil reached 40 mg/mL, the antioxidant value of the composite membrane was the highest. The reason may be that the improved active surface area and internal structure of the CH active film was uniform

and dense, with high stability, leading to continuous interaction and cooperation between chitosan and chestnut flower essential oil and a consequent superior ability to scavenge DPPH free radicals.

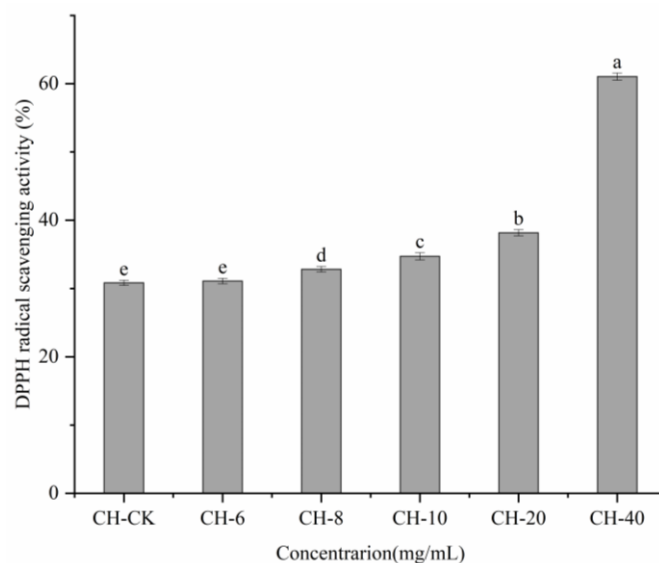


**Figure 4.** DPPH of composite films obtained with different concentrations of chestnut flower essential oil. The same letters are not significantly different at  $p < 0.05$ .

### 3.9. The Antibacterial and Antifungal Activities of Films

The antibacterial activity of CH-CK (with zero CFEO), CH-6 (with 6 mg/mL CFEO), CH-8 (with 8 mg/mL CFEO), CH-10 (with 10 mg/mL CFEO), CH-20 (with 20 mg/mL CFEO), and CH-40 (with 40 mg/mL CFEO) films was tested against Gram-negative (*E. coli*) and Gram-positive (*S. aureus*) bacteria. Figure 5 shows the antibacterial effect of the two bacteria exposed to the films. Compared to the chitosan blank membrane, when the concentration of chestnut flower essential oil reached 10 mg/mL, the film still had high bacteriostatic activity against *Staphylococcus aureus*. However, with a further increase in the chestnut flower essential oil concentration, the bacteriostatic effect of the film on *Staphylococcus aureus* declined, which may be due to the fact that when the concentration of CFEO increases, chitosan and the groups in chestnut flower essential oil are more firmly combined, resulting in the antibacterial components in the essential oil being difficult to release, and the bacteriostatic activity is correspondingly reduced. It is worth noting that compared with the bacteriostatic effect of *Staphylococcus aureus*, the antibacterial effect of the CH-CFEO complex membrane on *Escherichia coli* was significantly lower than that on *Staphylococcus aureus*. The main reason is that *E. coli* belong to Gram-negative bacteria, they have hard protective shell, and when their cell walls are disturbed, Gram-negative bacteria can enhance their resistance by changing their hydrophobic properties or by changing their outer membrane through mutations in pore proteins. In the case of *Staphylococcus aureus*, although they have a thicker peptidoglycan layer, they are more vulnerable to attack from the outside world due to the lack of an outer membrane. This is also the reason why the composite film showed different antibacterial effects on two bacteria. Therefore, this film exhibits increased protective barriers, possibly as a result of its antibacterial activity.

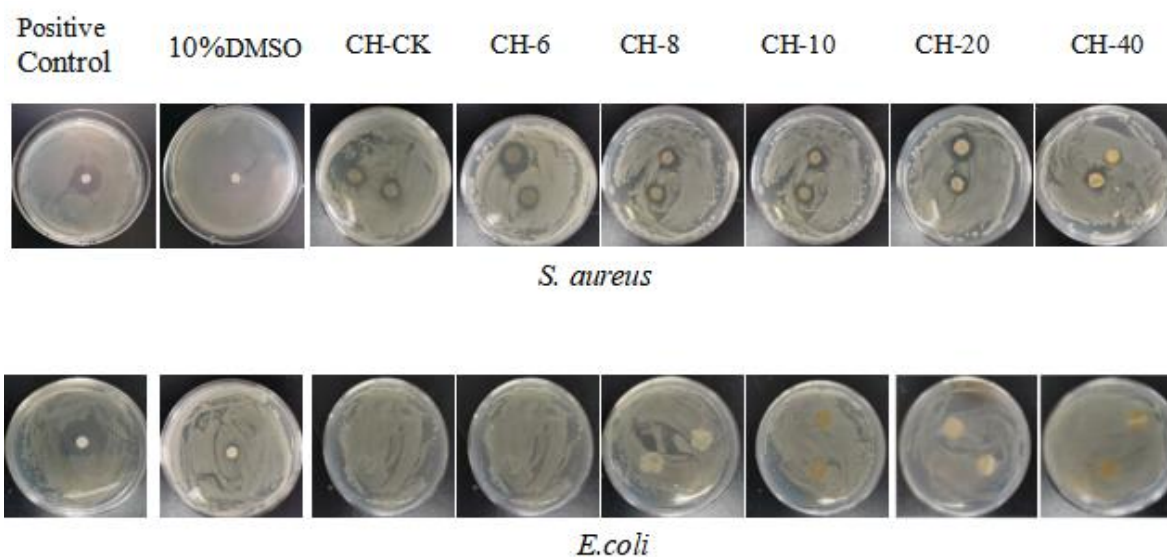


**Figure 5.** Antibacterial effect of chitosan–chestnut flower essential oil complex films on *S. aureus* and *E. coli*.

All tested CH-CFEO concentrations caused mycelial growth inhibition in *C. musae* isolates (Figure 6 and Table 2). CH (50  $\mu\text{g}/\text{mL}$ ) and CFEO (300, 600  $\mu\text{g}/\text{mL}$ ) caused MGI in the range of 12.19 to 48.85%, respectively. Moreover, the concentration of CH (100  $\mu\text{g}/\text{mL}$ ) and CFEO (300, 600  $\mu\text{g}/\text{mL}$ ) caused MGI in the range of 23.65 to 59.88%. These data indicate that the combinations of the lowest tested combined concentrations of CH (100  $\text{mg}/\text{mL}$ ) and CFEO (300, 600  $\mu\text{g}/\text{mL}$ ) have overall higher efficacy in inhibiting the target. The antifungal properties of CH have been commonly associated with interactions between positively charged CH molecules and negatively charged fungal cell membranes, causing alterations in membrane permeability and loss of electrolytes and other intracellular constituents important for fungal growth and survival [64–66]. CFEO (300, 600  $\mu\text{g}/\text{mL}$ ) also exerted inhibitory effects on the mycelial growth of all tested *C. musae* isolates. The results of these early investigations also revealed overall that the inhibitory effects on fungal growth increase when the EO concentrations increase [67–70]. Lundgren et al. investigated the antifungal effects of *Conyza bonariensis* (L.) Cronquist essential oil (CBEO) against pathogenic *Colletotrichum musae*. Coatings with CBEO (0.4–1  $\mu\text{L mL}^{-1}$ ) reduced anthracnose development in bananas artificially contaminated with *C. musae* during storage [71].

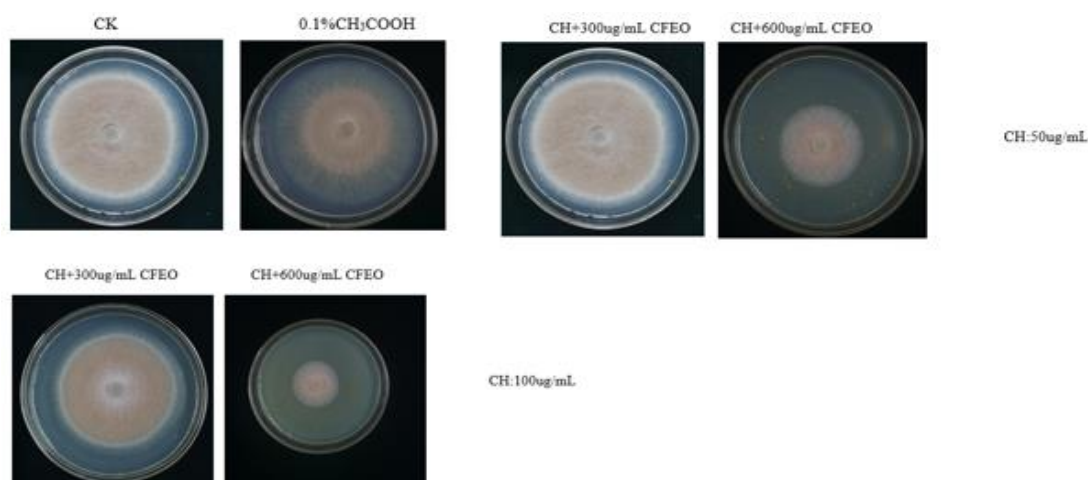


**Figure 6.** Inhibitory diameters at different concentrations of chitosan–chestnut flower essential oil against *C. musae*.

**Table 2.** Percentage of mycelial growth inhibition (MGI%) of *C. musae* after five-day exposure to different concentrations of chitosan (CH) and chestnut flower essential oil (CFEO) in a solid medium (25 °C). The same letters are not significantly different at  $p < 0.05$ .

CH (ug/mL)	CFEO (w/v)	MGI%
50	0.03	12.19 ± 0.02 <sup>d</sup>
	0.06	48.85 ± 0.00 <sup>b</sup>
100	0.03	23.65 ± 0.04 <sup>c</sup>
	0.06	59.88 ± 0.01 <sup>a</sup>

### 3.10. Effects on Banana Preservation

Figure 7 shows the effect of the composite films on the freshness of bananas. The control group clearly demonstrated that the bananas were significantly darkened and rotted on the sixth day. Meanwhile, for the groups with the CH-CK and CH-6, CH-8, CH-10, and CH-20 mg/mL films, significant spotting and darkening could also be observed. On the contrary, for the CH-40 mg/mL film, the least darkening and spoiling of bananas were observed, indicating a superior freshness preservation effect. Figure 7 shows the relationship between the weight loss rate of bananas and time; the weight loss rate of the composite films was close in the first day, and the lowest weight loss rate of the CH-40 mg/mL film could be observed on the sixth day. This could be explained by the relatively low water permeability and oxygen-blocking capability of the CH-40 mg/mL film, which provides multiple protective functions to reduce the weight loss of fruits and thus extend the shelf life of bananas. For the preservation effect of bananas, with the increase in the CFEO concentration, the film's UV resistance also increased; especially, when the concentration of CFEO reached 40 mg/mL, the film's ultraviolet resistance was the highest, which can be verified from the apparent form of bananas after 6 days, so the film with 40 mg/mL of chestnut flower essential oil can significantly extend the shelf life of bananas. In future research, banana preservation experiments under UV will be investigated.

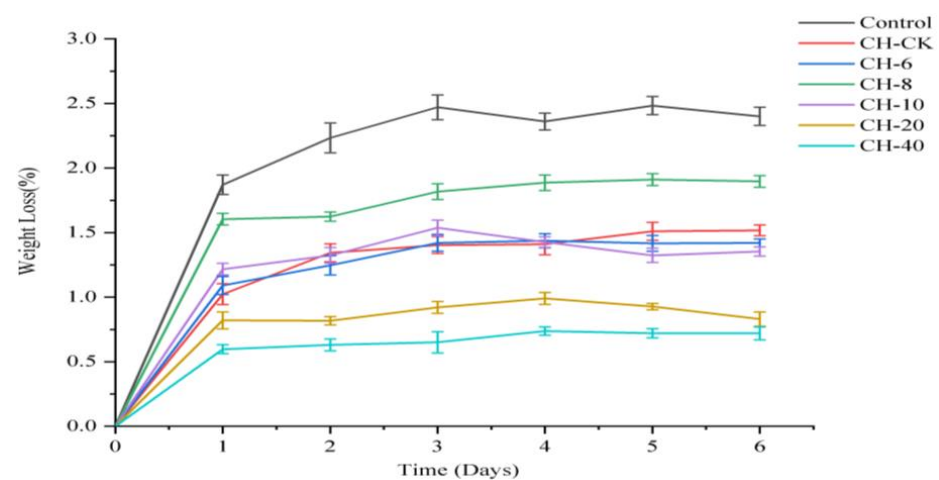


**Figure 7.** Cont.

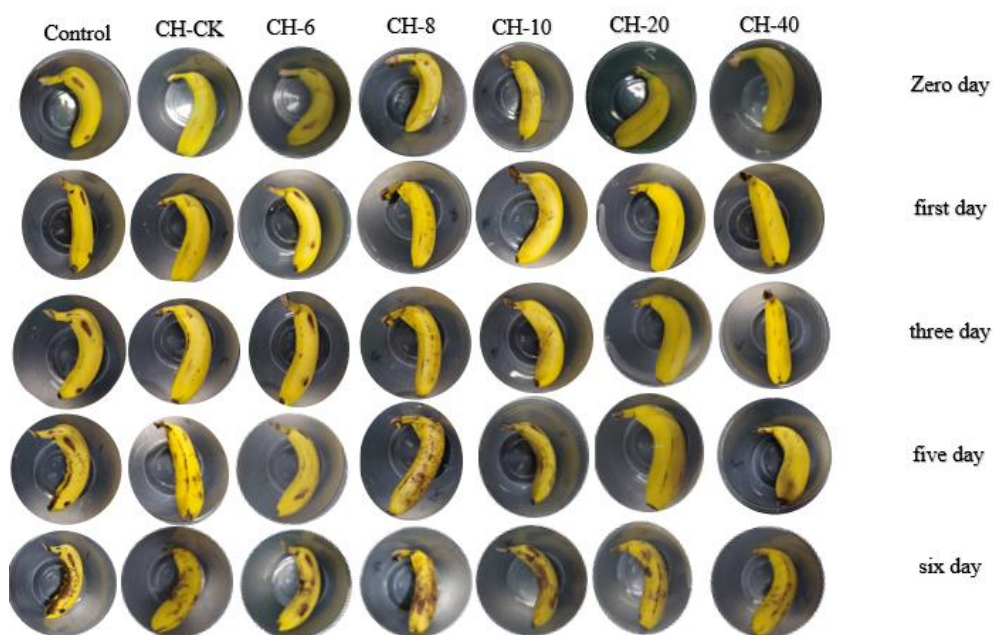


**Figure 7.** The fresh-keeping effect of chitosan–chestnut flower essential oil composite films with different concentrations on bananas.

#### 4. Conclusions

In summary, a CH-CFEO packaging film was prepared by the casting method. TGA tests showed that the addition of CFEO improves the heat resistance of the film. Antibacterial and antioxidant experiments also showed that the introduction of CFEO further improves the antibacterial and antioxidant properties of the film. Moreover, this film can prevent UV-induced spoilage of food and has the potential to be applied as food packaging. The CH-40 mg/mL film can significantly extend the shelf life of bananas due to its low water vapor permeability and effective antibacterial and oxidation resistance. Over a six-day storage period, the composite film slowed weight loss and enhanced banana hardness. Therefore, composite films have important prospects as an active packaging material with a variety of fruit and agricultural products' preservation and protection functions, which also provides an innovative example for the conversion of readily available natural biopolymers into profitable products that replace synthetic plastics and to meet the use of packaging film scenarios.

**Author Contributions:** Conceptualization, resources, methodology, data curation, writing—original draft: Y.L.; methodology, investigation, data curation, project administration: B.D.; methodology, investigation, validation: J.Z.; methodology, validation: F.P.; methodology, data curation, validation: K.N.; data curation, methodology, validation: W.H.; methodology, investigation: Y.Y. All authors have read and agreed to the published version of the manuscript.

**Funding:** This research was funded by Hebei province's key research and development program (216Z3201G).

**Institutional Review Board Statement:** Not applicable.

**Informed Consent Statement:** Not applicable.

**Data Availability Statement:** Data are contained within the article.

**Acknowledgments:** This work was technically supported by the Analysis and Testing Center, Hebei Normal University of Science and Technology.

**Conflicts of Interest:** We declare that the work has not been published elsewhere or considered by other journals. The manuscript is authorized by all authors to be submitted to the *International Journal of Biological Macromolecules*. The authors declare that they have no known competing financial interests or personal relationships that could affect the work reported in this paper.

## References

1. Basumatary, I.B.; Mukherjee, A.; Kumar, S. Chitosan-based composite films containing eugenol nanoemulsion, ZnO nanoparticles and *Aloe vera* gel for active food packaging. *Int. J. Biol. Macromol.* **2023**, *242*, 124826. [[CrossRef](#)]
2. Majumder, R.; Das, A.; Mukherjee, A.; Kumar, S. Biopolymers: The Chemistry of Food and Packaging. In *Biopolymer-Based Food Packaging: Innovations and Technology Applications*; John Wiley & Sons, Inc.: Hoboken, NJ, USA, 2022; pp. 29–65.
3. Kumar, S.; Mukherjee, A.; Dutta, J. (Eds.) *Biopolymer-Based Food Packaging: Innovations and Technology Applications*; John Wiley & Sons: Hoboken, NJ, USA, 2022.
4. Liu, J.; Liu, S.; Chen, Y.; Zhang, L.; Kan, J.; Jin, C. Physical, mechanical and antioxidant properties of chitosan films grafted with different hydroxybenzoic acids. *Food Hydrocoll.* **2017**, *71*, 176–186. [[CrossRef](#)]
5. Hamann, D.; Puton, B.M.S.; Colet, R.; Steffens, J.; Ceni, G.C.; Cansian, R.L.; Backes, G.T. Active edible films for application in meat products. *Res. Soc. Dev.* **2021**, *10*, 7. [[CrossRef](#)]
6. Najwa, I.; Guerrero, P.; Caba, K.; Hanani, Z. Physical and antioxidant properties of starch/gelatin films incorporated with *Garcinia atroviridis* leaves. *Food Packag. Shelf Life* **2020**, *26*, 100583. [[CrossRef](#)]
7. Rahman, P.M.; Mujeeb, V.M.A.; Muraleedharan, K. Flexible chitosan-nano ZnO antimicrobial pouches as a new material for extending the shelf life of raw meat. *Int. J. Biol. Macromol.* **2017**, *97*, 382–391. [[CrossRef](#)] [[PubMed](#)]
8. Dutta, P.K.; Tripathi, S.; Mehrotra, G.K.; Dutta, J. Perspectives for chitosan based antimicrobial films in food applications. *Food Chem.* **2009**, *114*, 1173–1182. [[CrossRef](#)]
9. Dordevic, S.; Dordevic, D.; Tesikova, K.; Sedlacek, P.; Kalina, M.; Vapenka, L.; Nejezchlebova, M.; Treml, J.; Tremlova, B.; Mikulášková, H.K. Nanometals incorporation into active and biodegradable chitosan films. *Heliyon* **2024**, *10*, e28430. [[CrossRef](#)] [[PubMed](#)]
10. Espitia, P.J.P.; Du, W.X.; Avena-Bustillos, R.D.J.; Soares, N.D.F.F.; Mchugh, T.H. Edible films from pectin: Physical-mechanical and antimicrobial properties—A review. *Food Hydrocoll.* **2014**, *35*, 287–296. [[CrossRef](#)]
11. Zhang, X.; Ismail, B.B.; Cheng, H.; Jin, T.Z.; Qian, M.; Arabi, S.A.; Liu, D.; Guo, M. Emerging chitosan-essential oil films and coatings for food preservation—A review of advances and applications. *Carbohydr. Polym.* **2021**, *273*, 118616. [[CrossRef](#)]
12. Dash, M.; Chiellini, F.; Ottenbrite, R.M.; Chiellini, E. Chitosan—A versatile semi-synthetic polymer in biomedical applications. *Prog. Polym. Sci.* **2011**, *36*, 981–1014. [[CrossRef](#)]
13. Cavallaro, G.; Micciulla, S.; Chiappisi, L.; Lazzara, G. Chitosan-based smart hybrid materials: A physico-chemical perspective. *J. Mater. Chem. B* **2021**, *9*, 94–611. [[CrossRef](#)] [[PubMed](#)]
14. Dai, W.; Zhou, L.; Gu, S.; Wang, W.; Xu, Z.; Zhou, X.; Ding, Y. Preparation and characterization of chitosan films incorporating epigallocatechin gallate: Microstructure, physicochemical, and bioactive properties. *Int. J. Biol. Macromol.* **2022**, *211*, 729–740. [[CrossRef](#)] [[PubMed](#)]
15. Kumar, S.; Mukherjee, A.; Dutta, J. Chitosan based nanocomposite films and coatings: Emerging antimicrobial food packaging alternatives. *Trends Food Sci. Technol.* **2020**, *97*, 196–209. [[CrossRef](#)]
16. Lisuzzo, L.; Cavallaro, G.; Milioto, S.; Lazzara, G. Layered composite based on halloysite and natural polymers: A carrier for the pH controlled release of drugs. *New J. Chem.* **2019**, *43*, 10887–10893. [[CrossRef](#)]
17. Ashrafi, A.; Jokar, M.; Nafchi, A.M. Preparation and characterization of biocomposite film based on chitosan and kombucha tea as active food packaging. *Int. J. Biol. Macromol.* **2018**, *108*, 444–454. [[CrossRef](#)] [[PubMed](#)]
18. Azeredo, H.M.C.; Morrugares-Carmona, R.; Wellner, N.; Cross, K.; Bajka, B.; Waldron, K.W. Development of pectin films with pomegranate juice and citric acid. *Food Chem.* **2016**, *198*, 101–106. [[CrossRef](#)] [[PubMed](#)]
19. Babaei-Ghazvini, A.; Shahabi-Ghahfarrokhi, I.; Goudarzi, V. Preparation of UV protective starch/kefiran/ZnO nanocomposite as a packaging film: Characterization. *Food Packag. Shelf Life* **2018**, *16*, 103–111. [[CrossRef](#)]
20. Chang, X.; Hou, Y.; Liu, Q.; Hu, Z.; Xie, Q.; Shan, Y.; Li, G.; Ding, S. Physicochemical and antimicrobial properties of chitosan composite films incorporated with glycerol monolaurate and nano-TiO<sub>2</sub>. *Food Hydrocoll.* **2021**, *119*, 106846. [[CrossRef](#)]
21. Zhao, H.; Zhu, Y.; Zhang, H.; Ren, H.; Zhai, H. UV-blocking composite films containing hydrophilized spruce kraft lignin and nanocellulose: Fabrication and performance evaluation. *Int. J. Biol. Macromol.* **2023**, *242*, 124946. [[CrossRef](#)]
22. Elshafie, H.S.; Camele, I. An overview of the biological effects of some mediterranean essential oils on human health. *BioMed Res. Int.* **2017**, *2017*, 9268468.
23. Mourey, A.; Canillac, N. Anti-listeria monocytogenes activity of essential oils components of conifers. *Food Control* **2002**, *13*, 289–292. [[CrossRef](#)]
24. Burt, S.A.; Reinders, R.D. Antibacterial activity of selected plant essential oils against *Escherichia coli* O157:H7. *Lett. Appl. Microbiol.* **2003**, *36*, 162–167. [[CrossRef](#)] [[PubMed](#)]
25. Božović, M.; Garzoli, S.; Sabatino, M.; Pepi, F.; Baldisserotto, A.; Andreotti, E.; Romagnoli, C.; Mai, A.; Manfredini Ragno, S.R. Essential oil extraction, chemical analysis and anti-*Candida* activity of *Calamintha nepeta* (L.) Savi subsp. *glandulosa* (Req.) ball-new approaches. *Molecules* **2017**, *22*, 203. [[CrossRef](#)] [[PubMed](#)]

26. Bae, Y.S.; Rhee, M.S. Short-term antifungal treatments of caprylic acid with carvacrol or thymol induce synergistic 6-log reduction of pathogenic candida albicans by cell membrane disruption and flux pump inhibition. *Cell. Physiol. Biochem.* **2019**, *53*, 285–300. [[PubMed](#)]
27. Anthony, J.P.; Fyfe, L.; Smith, H. Plant active components—A resource for antiparasitic agents? *Trends Parasitol.* **2005**, *21*, 462–468. [[CrossRef](#)]
28. Shahbazi, Y. The properties of chitosan and gelatin films incorporated with ethanolic red grape seed extract and *Ziziphora clinopodioides* essential oil as biodegradable materials for active food packaging. *Int. J. Biol. Macromol.* **2017**, *99*, 746–753. [[CrossRef](#)] [[PubMed](#)]
29. Wang, L.; Liu, F.; Jiang, Y.; Chai, Z.; Li, P.; Cheng, Y.; Jing, H.; Leng, X. Synergistic antimicrobial activities of natural essential oils with chitosan films. *J. Agric. Food Chem.* **2011**, *59*, 12411–12419. [[CrossRef](#)]
30. Ojagh, S.M.; Rezaei, M.; Razavi, S.H.; Hosseini, S.M.H. Development and evaluation of a novel biodegradable film made from chitosan and cinnamon essential oil with low affinity toward water. *Food Chem.* **2010**, *122*, 161–166. [[CrossRef](#)]
31. Liu, J.F.; Yang, Y.D.; Du, B.; Zhang, J.W.; Zhou, Y. Supercritical fluid extraction and GC-MS analysis of volatile oil from Chinese chestnut flower. *J. Hebei Norm Univ. Sci. Technol.* **2016**, *30*, 26–29. (In Chinese)
32. Vilaplana, R.; PazminO, L.; Valencia-Chamorro, S. Control of anthracnose, caused by *Colletotrichum musae*, on postharvest organic banana by thyme oil. *Postharvest Biol. Technol.* **2018**, *138*, 56–63. [[CrossRef](#)]
33. Yang, Z.; Li, M.; Zhai, X.; Zhao, L.; Tahir, H.E.; Shi, J.; Zou, X.; Huang, X.; Li, Z.; Xiao, J. Development and characterization of sodium alginate/tea tree essential oil nanoemulsion active film containing TiO<sub>2</sub> nanoparticles for banana packaging. *Int. J. Biol. Macromol.* **2022**, *213*, 145–154. [[CrossRef](#)] [[PubMed](#)]
34. ISO 527-2012; Plastics-Determination of tensile properties. International Standard: Geneva, Switzerland, 2012.
35. Liu, W.; Kang, S.; Zhang, Q.; Chen, S.; Yang, Q.; Yan, B. Self-assembly fabrication of chitosan-tannic acid/MXene composite film with excellent antibacterial and antioxidant properties for fruit preservation. *Food Chem.* **2023**, *410*, 135405. [[CrossRef](#)] [[PubMed](#)]
36. Zhang, L.; Zhang, Z.; Chen, Y.; Ma, X.; Xia, M. Chitosan and procyanidin composite films with high antioxidant activity and pH responsivity for cheese packaging. *Food Chem.* **2021**, *338*, 128013. [[CrossRef](#)] [[PubMed](#)]
37. Liu, J.; Liu, S.; Wu, Q.; Gu, Y.; Kan, J.; Jin, C. Effect of protocatechuic acid incorporation on the physical, mechanical, structural and antioxidant properties of chitosan film. *Food Hydrocoll.* **2017**, *73*, 90–100. [[CrossRef](#)]
38. Zhang, X.; Liu, Y.; Yong, H.; Qin, Y.; Liu, J.; Liu, J. Development of multifunctional food packaging films based on chitosan, TiO<sub>2</sub> nanoparticles and anthocyanin-rich black plum peel extract. *Food Hydrocoll.* **2019**, *94*, 80–92. [[CrossRef](#)]
39. Da Silva, D.C.; Lopes, I.A.; Da Silva, L.J.S.; Lima, M.F.; Barros Filho, A.K.D.; VillaV´elez, H.A.; Santana, A.A. Physical properties of films based on pectin and babassu coconut mesocarp. *Int. J. Biol. Macromol.* **2019**, *130*, 419–428. [[CrossRef](#)] [[PubMed](#)]
40. Al-Maqtari, Q.A.; Al-Gheethi, A.A.; Ghaleb, A.D.; Mahdi, A.A.; Al-Ansi, W.; Noman, A.E.; Al-Adeeb, A.; Odjo, A.K.; Du, Y.; Wei, M.; et al. Fabrication and characterization of chitosan/gelatin films loaded with microcapsules of *Pulicaria jaubertii* extract. *Food Hydrocoll.* **2022**, *129*, 107624. [[CrossRef](#)]
41. Alam, T.; Asif, S.; Ayaz, S.; Rehman, H.; Sana, A.; Alam, S.; Qamar, F.; Naveed, S.; Ghi, A.O. Total phenolic content and total flavonoid content of *Embelia ribes* by radical scavenging activity. *Lat. Am. J. Pharm.* **2019**, *38*, 1467–1471.
42. Dos Passos Braga, S.; Lundgren, G.A.; Macedo, S.A.; Tavares, J.F.; Dos Santos Vieira, W.A.; Câmara, M.P.S.; de Souza, E.L. Application of coatings formed by chitosan and *Mentha* essential oils to control anthracnose caused by *Colletotrichum gloeosporioides* and *C. brevisporum* in papaya (*Carica papaya* L.) fruit. *Int. J. Biol. Macromol.* **2019**, *139*, 631–639. [[CrossRef](#)]
43. Lei, Y.; Wu, H.; Jiao, C.; Jiang, Y.; Liu, R.; Xiao, D.; Lu, J.; Zhang, Z.; Shen, G.; Li, S. Investigation of the structural and physical properties, antioxidant and antimicrobial activity of pectin-konjac glucomannan composite edible films incorporated with tea polyphenol. *Food Hydrocoll.* **2019**, *94*, 128–135. [[CrossRef](#)]
44. Chen, Y.; Li, Y.; Qin, S.; Han, S.; Qi, H. Antimicrobial, UV blocking, water-resistant and degradable coatings and packaging films based on wheat gluten and lignocellulose for food preservation. *Composites* **2022**, *238*, 109868. [[CrossRef](#)]
45. Zhang, Y.Y.; Yang, Y.; Tang, K.; Hu, X.; Zou, G.L. Physicochemical characterization and antioxidant activity of quercetin-loaded chitosan nanoparticles. *J. Appl. Polym. Sci.* **2008**, *107*, 891–897. [[CrossRef](#)]
46. Halasz, K.; Csóka, L. Black chokeberry (*Aronia melanocarpa*) pomace extract immobilized in chitosan for colorimetric pH indicator film application. *Food Packag. Shelf Life* **2018**, *16*, 185–193. [[CrossRef](#)]
47. Wang, L.Y.; Guo, H.Y.; Wang, J.; Jiang, G.C.; Du, F.H.; Liu, X.J. Effects of *Herba lophatheri* extract on the physicochemical properties and biological activities of the chitosan film. *Int. J. Biol. Macromol.* **2019**, *133*, 51–57. [[CrossRef](#)]
48. Uranga, J.; Puertas, A.I.; Etxabide, A.; Dueñas, M.T.; Guerrero, P.; de la Caba, K. Citric acid incorporated fish gelatin/chitosan composite films. *Food Hydrocoll.* **2019**, *86*, 95–103. [[CrossRef](#)]
49. Rui, L.; Min, H.X.; Bing, H.; Li, Z.; Dan, Y.Y.; Xiao, X.Z. A comparative study on chitosan/gelatin composite films with conjugated or incorporated gallic acid. *Carbohydr. Polym.* **2017**, *173*, 473–481. [[CrossRef](#)]
50. Díaz-Montes, E.; Ya´nez-Fernandez, J.; Castro-Munoz, R. Dextran/chitosan blend film fabrication for bio-packaging of mushrooms (*Agaricus bisporus*). *J. Food Process Preserv.* **2021**, *45*, e15489. [[CrossRef](#)]
51. Fabra, M.J.; Falcó, I.; Randazzo, W.; Sánchez, G.; López-Rubio, A. Antiviral and antioxidant properties of active alginate edible films containing phenolic extracts. *Food Hydrocoll.* **2018**, *81*, 96–103. [[CrossRef](#)]
52. Lawrie, G.; Keen, I.; Drew, B.; Chandler-Temple, A.; Rintoul, L.; Fredericks, P.; Grøndahl, L. Interactions between alginate and chitosan biopolymers characterized using FTIR and XPS. *Biomacromolecules* **2007**, *8*, 2533–2541. [[CrossRef](#)]

53. Qiao, C.; Ma, X.; Zhang, J.; Yao, J. Molecular interactions in gelatin/chitosan composite films. *Food Chem.* **2017**, *235*, 45–50. [[CrossRef](#)]
54. Raphaël, K.J.; Meimandipoour, A. Antimicrobial activity of chitosan film forming solution enriched with essential oils; an in Vitro Assay. *Iran. J. Biotechnol.* **2017**, *15*, 111–119. [[PubMed](#)]
55. Zhang, L.; Li, K.; Yu, D.; Regenstein, J.M.; Dong, J.; Chen, W.; Xia, W. Chitosan/zein bilayer films with one-way water barrier characteristic: Physical, structural and thermal properties. *Int. J. Biol. Macromol.* **2022**, *200*, 378–387. [[CrossRef](#)] [[PubMed](#)]
56. Li, Y.; Chen, Y.; Wu, Q.; Huang, J.; Zhao, Y.; Li, Q.; Wang, S. Improved Hydrophobic, UV Barrier and Antibacterial Properties of Multifunctional PVA Nanocomposite Films Reinforced with Modified Lignin Contained Cellulose Nanofibers. *Polymers* **2022**, *14*, 1705. [[CrossRef](#)]
57. Dou, J.; Vuorinen, T.; Koivula, H.; Forsman, N.; Sipponen, M.; Hietala, S. Self-standing lignin-containing willow bark nanocellulose films for oxygen blocking and UV shielding. *ACS Appl. Nano Mater.* **2021**, *4*, 2921–2929. [[CrossRef](#)]
58. Cao, T.L.; Song, K.B. Effects of gum karaya addition on the characteristics of loquat seed starch films containing oregano essential oil. *Food Hydrocoll.* **2019**, *97*, 105198. [[CrossRef](#)]
59. Riaz, A.; Lei, S.; Akhtar, H.M.S.; Wan, P.; Chen, D.; Jabbar, S.; Abid, M.; Hashim, M.M.; Zeng, X. Preparation and characterization of chitosan-based antimicrobial active food packaging film incorporated with apple peel polyphenols. *Int. J. Biol. Macromol.* **2018**, *114*, 547–555. [[CrossRef](#)] [[PubMed](#)]
60. Ren, M.; Cai, Z.; Chen, L.; Wa, H.; Zhang, L.; Wang, Y.; Yu, X.; Zhou, C. Preparation of zein/chitosan/eugenol/curcumin active films for blueberry preservation. *Int. J. Biol. Macromol.* **2022**, *223*, 1054–1066. [[CrossRef](#)] [[PubMed](#)]
61. Tessaro, L.; Luciano, C.G.; Quinta Barbosa Bittante, A.M.; Lourenço, R.V.; MartelliTosi, M.; Jos´e do Amaral Sobral, P. Gelatin and/or chitosan-based films activated with “Pitanga” (*Eugenia uniflora* L.) leaf hydroethanolic extract encapsulated in double emulsion. *Food Hydrocoll.* **2021**, *113*, 106523. [[CrossRef](#)]
62. Roy, S.; Rhim, J.W. Fabrication of bioactive binary composite film based on gelatin/chitosan incorporated with cinnamon essential oil and rutin. *Colloids Surf. B Biointerfaces* **2021**, *204*, 111830. [[CrossRef](#)]
63. Qin, Y.; Liu, Y.; Yuan, L.; Yong, H.; Liu, J. Preparation and characterization of antioxidant, antimicrobial and pH-sensitive films based on chitosan, silver nanoparticles and purple corn extract. *Food Hydrocoll.* **2019**, *96*, 102–111. [[CrossRef](#)]
64. Benbettaieb, N.; Tanner, C.; Cayot, P.; Karbowiak, T.; Debeaufort, F. Impact of functional properties and release kinetics on antioxidant activity of biopolymer active films and coatings. *Food Chem.* **2018**, *242*, 369–377. [[CrossRef](#)] [[PubMed](#)]
65. Guerra, I.C.D.; de Oliveira, P.D.L.; de Souza Pontes, A.L.; Lúcio, A.S.S.C.; Tavares, J.F.; Barbosa-Filho, J.M.; Madruga, M.S.; de Souza, E.L. Coatings comprising chitosan and *Mentha piperita* L. or *Mentha × villosa* Huds essential oils to prevent common postharvest mold infections and maintain the quality of cherry tomato fruit. *Int. J. Food Microbiol.* **2015**, *214*, 168–178. [[CrossRef](#)]
66. de Oliveira, K.Á.R.; Berger, L.R.R.; de Araújo, S.A.; Câmara, M.P.S.; de Souza, E.L. Synergistic mixtures of chitosan and *Mentha piperita* L. essential oil to inhibit *Colletotrichum* species and anthracnose development in mango cultivar Tommy Atkins. *Food Microbiol.* **2017**, *66*, 96–103. [[CrossRef](#)] [[PubMed](#)]
67. Munhuweyi, K.; Caleb, O.J.; Lennox, C.L.; van Reenen, A.J.; Opara, U.L. In vitro and in vivo antifungal activity of chitosan-essential oils against pomegranate fruit pathogens. *Postharvest Biol. Technol.* **2017**, *129*, 9–22. [[CrossRef](#)]
68. Santos, N.S.T.D.; Athayde Aguiar, A.J.A.; Oliveira, C.E.V.D. Efficacy of the application of a coating composed of chitosan and *Origanum vulgare* L. essential oil to control *Rhizopus stolonifer* and *Aspergillus niger* in grapes (*Vitis labrusca* L.). *Food Microbiol.* **2012**, *32*, 345–353. [[CrossRef](#)] [[PubMed](#)]
69. Monzón-Ortega, K.; Salvador-Figueroa, M.; Gálvez-López, D.; Rosas-Quijano, R.; Ovando-Medina, I.; Vázquez-Ovando, A. Characterization of *Aloe vera*-chitosan composite films and their use for reducing the disease caused by fungi in papaya Maradol. *J. Food Sci. Technol.* **2018**, *55*, 4747–4757. [[CrossRef](#)]
70. Xu, D.; Qin, H.R.; Ren, D. Prolonged preservation of tangerine fruits using chitosan/montmorillonite composite coating. *Postharvest Biol. Technol.* **2018**, *143*, 50–57. [[CrossRef](#)]
71. Lundgren, G.A.; Braga, S.D.P.; de Albuquerque, T.M.R.; Árabe Rimá de Oliveira, K.; Tavares, J.F.; Vieira, W.A.D.S.; Câmara, M.P.S.; de Souza, E.L. Antifungal effects of *Conyza bonariensis* (L.) Cronquist essential oil against pathogenic *Colletotrichum musae* and its incorporation in gum Arabic coating to reduce anthracnose development in banana during storage. *J. Appl. Microbiol.* **2022**, *132*, 547–561. [[CrossRef](#)]

**Disclaimer/Publisher’s Note:** The statements, opinions and data contained in all publications are solely those of the individual author(s) and contributor(s) and not of MDPI and/or the editor(s). MDPI and/or the editor(s) disclaim responsibility for any injury to people or property resulting from any ideas, methods, instructions or products referred to in the content.